Journal of Petroleum Science and Technology 10 (2020) 1-11
DOI:10.22078/jpst.2020.4066.1652

Journal of Petroleum Science and Technology

https://jpst.ripi.ir/

Entropy Analysis within Rotating Cylinders of Annulus for Giesekus Viscoelastic Fluid

Mehdi Moayed Mohseni
Department of Chemical Engineering, Amirkabir University of Technology, Tehran, Iran

Abstract
Entropy analysis, along with convective heat transfer within rotating cylinders of the annulus, is presented using a purely analytical approach for Giesekus rheological model. Two different types of boundary conditions are considered: (a) the constant and different temperature at walls, (b) constant heat flux at the outer wall, and constant temperature at the inner wall. Also, the derived velocity and temperature profiles are coupled in the entropy equation for obtaining the volumetric entropy-generation and the Bejan number expressions. Moreover, the effects of Deborah number (De), mobility factor (α), group parameter (Br/Ω), Brinkman number (Br), and velocity ratio (β) on the above parameters are investigated. Ultimately, results indicate that increment of Brinkman number and group parameters increases irreversibility except when both cylinders rotate with identical angular velocity in the same direction.

Key words: Entropy Generation, Giesekus Constitutive Equation, Bejan Number, Analytical Solution, Rotating Cylinders.

Introduction
Cylindrical annular space geometry is frequently encountered in industry and engineering equipment such as electronic packages, electrical equipment, industrial heat exchangers, and petroleum drilling equipment [1]. Therefore, the annular flow geometry has always been investigated in many studies from the past to the present [1-9].

The flow that is induced by relative rotating motion inside an annulus has many engineering applications such as in the swirl nozzles, chemical and mechanical mixing equipment, journal bearings, electrical motors, and commercial viscometers [10]. A nonlinear viscoelastic model using molecular ideas based on three-parameters of the relaxation, retardation times, and a mobility factor, has been developed by Giesekus [11]. This model has advantages over many other models. For example, this model can describe the reasonable complex and elongational viscosity or power-law regions for viscosity and normal-stress coefficients. It can also predict the shear thinning and shear viscosity, non-exponential stress relaxation, finite asymptotic value for extensional viscosity, and start-up curves. Therefore, many rheological characteristics of polymeric solutions and other liquids could be reproduced by the Giesekus model.

The hydrodynamics and convective heat transfer of Giesekus fluid in an annulus with both cylinder rotation are done by Jouyandeh et al. [12,13]. The analytical equations of viscometric functions were derived, and their solutions compared with experimental data [12]. Their results showed that the viscometric functions decreased by increasing the elasticity of fluid. Also, in the other work which has been carried out by them [13], the convective heat transfer of this problem for isothermal boundary conditions by pure analytical method was investigated. Also, for the constant temperature boundary conditions, two cases of different and identical wall temperatures were considered. According to the study, it was found out that the Nusselt number was independent of viscous dissipation for the identical wall temperature case.

Cost reduction is the main objective of the engineering system, and enhancement of thermodynamics efficiency means optimizing the system economically. For this purpose, the rate of thermodynamics irreversibility or the lost available work ($\dot{I}$) should be reduced. Moreover, lost available work ($\dot{I}$) is obtained using the following equation (Equation 1) [14]:

$$\dot{I} = W_{rev} - W_{real}, \quad (1)$$

The thermodynamics irreversibility rate is a direct function of the entropy generation rate that can be

*Corresponding author: Mehdi Moayed Mohseni, *Department of Chemical Engineering, Amirkabir University of Technology, Tehran, Iran*
E-mail addresses: m.moayed.@aut.ac.ir
Received 2020-01-30, Received in revised form 2020-07-23, Accepted 2020-08-05, Available online 2020-11-22

obtained by [14]:

$$\dot{I} = T_{ref}\dot{S}_{gen}. \quad (2)$$

Therefore, the thermodynamics irreversibility decreases with the reduction of entropy generation rate, and the system will be optimized. Entropy is generated in all heat transfer systems. Furthermore, different sources cause the generation of entropy, such as heat transfer across a finite temperature gradient, characteristics of convective heat transfer, and viscous effects. In this respect, the entropy generation number and irreversibility distribution ratio were introduced in "fundamental convective heat transfer" by Bejan [15]. Also, the second-law analysis in heat transfer and thermal design for minimizing irreversibility is investigated by Bejan [16]. Analysis of entropy in a concentric annulus with outer cylinder rotation and different constant temperature boundary conditions was presented by Yilbas [17] for a Newtonian fluid. Moreover, the second law analysis in rotating cylinders annuli for the Newtonian fluid was studied by Mahmud and Fraser [18,19] analytically. In addition, both isoflux and isothermal boundary conditions were used by them. Furthermore, the entropy generation in channel and pipe for non-Newtonian fluids with isoflux boundary conditions was also analyzed by them [20]. The analytical expressions for velocity, temperature, and entropy generation were derived in rotating annulus by Mahian et al. [21] for MHD flow with isothermal boundary conditions. Also, similar problems but for mixed convection and both isoflux and isothermal boundary conditions were solved by Mahian et al. [22,23]. For non-Newtonian fluid, entropy analysis in rotating annulus for a third-grade fluid with isoflux boundary conditions and using the perturbation method was presented by Kahraman and Yurusoy [24]. Also, for a third-grade fluid, entropy generation in a fully developed axial annular flow with isothermal boundary conditions was studied by Yilbas et al. [25]. Also, this problem was carried out with variable viscosity by Yurusoy et al. [26]. Second law analysis for viscoelastic fluid is scarce. The analytical expressions for temperature, entropy generation number and Bejan number with isothermal and isoflux boundary conditions for sPTT viscoelastic fluid in rotating cylinders were obtained by Mirzazadeh et al. [27]. Also, the entropy analysis for Giesekus viscoelastic fluid was investigated by Moayed and Rashidi [28]. In addition, a fully axial annular flow using an analytical approach was developed for both isothermal and isoflux thermal boundary conditions by them. . Furthermore, a mathematical model by homotopy perturbation method for Jeffery viscoelastic nanofluid passing in an eccentric asymmetric annuli was developed by Riaz et al [6]. In addition to heat transfer, mass transfer is also effective in the entropy generation in their model. The entropy generation on the asymmetric peristaltic propulsion for Williamson non-Newtonian fluid was also investigated by Riaz et al [29]. Moreover, the presented model is formulated under the approximation of small Reynolds number and long wavelength ofthe peristaltic wave. A regular perturbation method for solving momentum and heat transfer equations was employed by them. To the best of our knowledge, the second law analysis for Giesekus fluid in rotating annulus with both cylinders' rotation has not been yet investigated. Hence, an analytical approach to this problem in the present study was presented. The governing equations of momentum and energy in the presence of viscous dissipation are solved analytically, and subsequently, the expressions for non-dimensional entropy generation number due to fluid friction and heat transfer, irreversibility distribution ratio, and Bejan number are derived.

The first and fourth kinds of thermal boundary conditions are considered in this study. In the case of the first kind, the temperatures at both the walls are constant, for example, in a two-fluid heat exchanger when the phase-change (boiling or condensation) occurs at both tubes. In the case of the fourth kind, one constant wall heat flux is specified, and the other wall is at a constant temperature. If one of the tubes undergoes the phase change, and on the other, one of the fluid flows has the same capacity rate with thin-walled tubes, the thermal boundary conditions will be the fourth kind. These thermal boundary conditions are common in the many thermal processing applications; therefore, they have been employed in extensive studies [19,27,30-32].

Physical Model and Mathematical Formulation

The schematic of the problem under investigation is shown in Fig.1. The flow is considered to be steady-state, laminar, and purely tangential in a concentric annulus. Relative rotational motion between both cylinders induces the flow. The outer and inner cylinder radiuses are shown respectively with Ro and R_i, Π is the radius ratio (R_o/R_i), and the annular gap is defined as $\delta=R_i(\Pi-1)$.

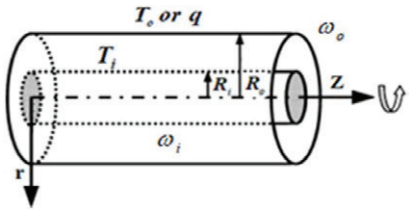

Fig. 1 Schematic view of an annular under consideration.

Two different cases of boundary conditions are considered as below:

$$r = R_i, \qquad V_\theta = R_i\omega_i, \qquad T = T_i, \quad (3)$$

$$r = R_o, \qquad V_\theta = R_o\omega_o, \qquad T = T_o, \quad \text{or} \quad \frac{\partial T}{\partial r} = \frac{q_o}{k}. \quad (4)$$

ω_i and ω_0 are the inner and outer wall angular velocity respectively.

The energy equation by assuming viscous dissipation and neglecting axial heat conduction can be written as:

$$\frac{k}{r}\frac{\partial}{\partial r}\left(r\frac{\partial T}{\partial r}\right) + \tau_{r\theta}\, r\frac{d}{dr}\left(\frac{V_\theta}{r}\right) = 0, \quad (5)$$

By employing non-dimensional quantities, the energy equation can be written as follows:

$$\frac{1}{R^*}\frac{\partial}{\partial R^*}\left(R^*\frac{\partial \Theta}{\partial R^*}\right) + \frac{Br}{\Pi - 1}\tau^*_{r\theta}R^*\frac{\partial}{\partial R^*}\left(\frac{V^*_\theta}{R^*}\right) = 0. \quad (6)$$

The hydrodynamic non-dimensional quantities are as follows:

$$R^* = \frac{r}{R_i}, \quad .. \qquad V^*_\theta = \frac{V_\theta}{u_c}, \qquad \tau^*_{r\theta} = \frac{\tau_{r\theta}}{\eta u_c/\delta},$$

where uc is the characteristic velocity of the inner cylinder ($u_c = R_i\omega_i$).

The thermal non-dimensional quantities are different between the two thermal boundary conditions.

where both cylinders are isothermal, the non-dimensional temperature and Brinkman number are as follows:

$$\Theta = \frac{T - T_i}{T_o - T_i}, \quad (7a) \qquad Br = \frac{\eta u_c^{\,2}}{k(T_o - T_i)}, \quad (7b)$$

And where the outer cylinder is isoflux, and the inner cylinder is isothermal, these non-dimensional quantities are as follows:

$$\Theta = \frac{T - T_i}{q/R_i\, k}, \quad (7c) \qquad Br = \frac{\eta u_c^{\,2}}{qR_i}. \quad (7d)$$

Br is the Brinkman number, which is a measure of the importance of the viscous dissipation.

Also, the non-dimensional form of boundary conditions can be written as follows:

$$R^* = 1, \qquad V_\theta^* = 1, \qquad \Theta = 0, \quad (8a)$$

$$R^* = \Pi, \qquad V_\theta^* = \beta, \qquad \Theta = 1, \text{ or } \quad \frac{\partial \Theta}{\partial R^*} = 1. \quad (8b)$$

β is velocity ratio and defined as the velocity at the outer cylinder to the inner cylinder, $\beta = R_o\omega_o / R_i\omega_i$

Analytical Solution

Hydrodynamics constitutive equation

The Giesekus model, which is used as a rheological model is:

$$\tau + \frac{\alpha\lambda}{\eta}(\tau.\tau) + \lambda\tau_{(1)} = 2\eta D, \quad (9)$$

where

$$2D = \dot{\gamma} = [\nabla\upsilon + (\nabla\upsilon)^T], \quad (10)$$

$$\tau_{(1)} = \frac{\vartheta\tau}{\vartheta t} = \frac{D\tau}{Dt} - \{\tau.\nabla\upsilon + (\nabla\upsilon)^T.\tau\}, \quad (11)$$

$$\frac{D\tau}{Dt} = \frac{\partial\tau}{\partial t} + (\upsilon.\nabla)\tau. \quad (12)$$

τ, λ and η are the stress tensor, zero shear relaxation time, and zero shear viscosity respectively [33]. Also, α is another model parameter which is called mobility factor and represents anisotropic Brownian motion and/or anisotropic hydrodynamic drag on the constituent polymer molecules [34]. Giesekus [11] discuses about and shows it is required that $0 \le \alpha \le 1$

Hydrodynamic Solution

The non-dimensional form of momentum equation could be

$$(\Pi - 1)R^* \frac{\partial}{\partial R^*}\left(\frac{V_\theta^*}{R^*}\right) = \frac{1 + (2\alpha - 1)De\,\tau_{rr}^*}{(1 + De\,\tau_{rr}^*)^2}\tau_{r\theta}^*, \quad (13)$$

By integrating from Eq. (13), the velocity profile is derived as:

$$\frac{V_\theta^*}{R^*} = \frac{\tau_{wi}^*}{\Pi - 1}\left(\frac{R^{*2}(\alpha - 1)}{2(R^{*4} - \alpha De^2 \tau_{wi}^{*\,2})} - \frac{\sqrt{\alpha}\,\arctan h\left(\frac{R^{*2}}{\sqrt{\alpha}De\tau_{wi}^*}\right)}{2De\tau_{wi}^*}\right) + C_1. \quad (14)$$

where C_1 is the constant of integration and is obtained by putting boundary condition Eq. (8-a) in Eq. (14) as follows:

$$C_1 = 1 - \frac{\tau_{wi}^*}{\Pi - 1}\left(\frac{\alpha - 1}{2(1 - \alpha De^2 \tau_{wi}^{*\,2})} - \frac{\sqrt{\alpha}\,\arctan h\left(\frac{1}{\sqrt{\alpha}De\tau_{wi}^*}\right)}{2De\tau_{wi}^*}\right), \quad (15)$$

And shear stress $\tau_{r\theta}^*$ is derived [12] in as follows:

$$\tau_{r\theta}^* = \frac{\tau_{wi}^*}{R^{*2}}. \quad (16)$$

In these equations, De is the Deborah number that is defined as ($\lambda u_c/\delta$), and De represents the level of fluid elasticity and τ_{wi}^* is non-dimensional shear stress on the inner wall of the annulus.

For a Newtonian fluid, the following equations are obtained by Mahmud and Fraser [19]:

$$\frac{V_\theta^*}{R^*} = -\frac{\tau_{wi}^*}{2R^{*2}(\Pi - 1)} + C_1, \quad (17)$$

$$\tau_{wi}^* = -\frac{2\Pi(\Pi - \beta)}{\Pi + 1}, \quad (18)$$

$$C_1 = 1 + \frac{\tau_{wi}^*}{2(\Pi - 1)}. \quad (19)$$

If α and De tend to zero then the rheological properties of Giesekus fluid is approaching the Newtonian.

First Law Analysis

By substituting velocity profile and shear stress from Eqs. (14 and 16) in Eq. (6) and then integrating them, the following expression for non-dimensional temperature is obtained:

$$\Theta = \frac{\sqrt{\alpha}Br\tau_{wi}^*}{8De(\Pi - 1)^2}\left[\text{PolyLog}\left(2, \frac{R^{*2}}{X}\right) - \text{PolyLog}\left(2, -\frac{R^{*2}}{X}\right)\right]$$

$$-\frac{Br\tau_{wi}^*(\alpha - 1)}{8\sqrt{\alpha}De(\Pi - 1)^2}\text{Log}\left(\frac{R^{*2} - X}{R^{*2} + X}\right) + C_2\text{Log}(R^*) + C_3. \quad (20)$$

where $X = \sqrt{\alpha}De_{wi}^*$ and C_2 and C_3 are Integral constants which can be obtained by imposing boundary conditions as follows:

$$C_{2T} = -\frac{C_3 - 1}{\text{Log}(\Pi)} + \frac{Br\tau_{wi}^*[(\alpha - 1)\text{Log}(\frac{\Pi^2 - X}{\Pi^2 + X}) + \alpha(\text{PolyLog}[2, -\frac{\Pi^2}{X}] - \text{PolyLog}[2, \frac{\Pi^2}{X}])]}{8\sqrt{\alpha}De(\Pi - 1)^2\text{Log}(\Pi)}, \quad (21)$$

$$C_{3T} = -\frac{Br\tau_{wi}^*}{8\sqrt{\alpha}De(\Pi - 1)^2} \times \left[(\alpha - 1)\text{Log}\left(\frac{1 - X}{1 + X}\right) + \alpha\text{PolyLog}\left(2, -\frac{1}{X}\right) - \alpha\text{PolyLog}\left(2, \frac{1}{X}\right)\right], \quad (22)$$

$$C_{2q} = \Pi\left[1 + \frac{Br\tau_{wi}^{*\,2}}{2\Pi(\Pi - 1)^2}\left(\frac{\Pi^2(\alpha - 1)}{\Pi^4 - X^2} - \frac{\sqrt{\alpha}\,\arctan h\left(\Pi^2/X\right)}{De\tau_{wi}^*}\right)\right], \quad (23)$$

$$C_{3q}=\frac{Br\tau^{*}_{wi}}{8\sqrt{\alpha}De(\Pi-1)^{2}}$$
$$\left[(\alpha-1)Log\left(\frac{1-X}{1+X}\right)+\alpha PolyLog\left(2,-\frac{1}{X}\right)-\alpha PolyLog\left(2,\frac{1}{X}\right)\right]. \quad (24)$$

For the Newtonian fluid (α and De=0), Θ and its constants for the two types of boundary conditions become as follows (Equations 25 to 27) [27]:

$$\Theta_{N}=-\frac{Br\Pi\tau^{*}_{wi}(\beta-\Pi)}{2R^{*}(\Pi+1)(\Pi-1)^{2}}+C_{2}Log\left(R^{*}\right)+C_{3}. \quad (25)$$

$$C_{2T}=\frac{-1-Br\beta^{2}+2Br\beta\Pi+\Pi^{2}-Br\Pi^{2}}{(\Pi^{2}-1)Log(\Pi)},$$
$$C_{3T}=\frac{Br\Pi^{2}(\beta-\Pi)^{2}}{(\Pi^{2}-1)^{2}}, \quad (26)$$

$$C_{2q}=\frac{\Pi^{2}-\Pi^{3}-\Pi^{4}+\Pi^{5}-Br\beta\tau^{*}_{wi}+Br\Pi\tau^{*}_{wi}}{\Pi(\Pi+1)(\Pi-1)^{2}},$$
$$C_{3q}=\frac{Br\Pi\tau^{*}_{wi}(\beta-\Pi)}{(\Pi+1)(\Pi-1)^{2}}. \quad (27)$$

Second Law Analysis

The general equation for the entropy generation per unit volume SG (Wm-3k-1) is given by Bejan [35]:

$$S_{G}=\frac{k}{T_{i}^{2}}(\nabla T)^{2}+\frac{\Phi}{T_{i}}, \quad (28)$$

The viscous dissipation term (Φ) is defined as:

$$\Phi=\tau_{r\theta}r\frac{d}{dr}\left(\frac{V_{\theta}}{r}\right), \quad (29)$$

By substituting from Eq. (29) into Eq. (28), the entropy can be obtained as following form:

$$S_{G}=\frac{k}{T_{i}^{2}}\left(\frac{dT}{dr}\right)^{2}+\frac{\tau_{r\theta}}{T_{i}}r\frac{d}{dr}\left(\frac{V_{\theta}}{r}\right). \quad (30)$$

The terms of Eq. (30) from left to right represent entropy generation due to the heat transfer and the viscous dissipation respectively. To better illustrate the problem, the non-dimensional entropy generation number (N_s) is employed. The entropy generation number is the ratio of volumetric entropy generation and the characteristic entropy generation ($S_{G,c}$). According to Bejan [15, 16], the characteristic entropy generation ($S_{G,c}$) for isothermal and isoflux conditions are:

$$S_{G,c}=\left[\frac{k(T_{o}-T_{i})}{r_{i}^{2}T_{i}^{2}}\right]_{Isothermal}, \qquad S_{G,c}=\left[\frac{q^{2}}{kT_{i}^{2}}\right]_{Isoflux}, \quad (31)$$

The relevant definition for entropy generation number is:

$$N_{s}=\frac{S_{G}}{S_{G,c}}=\left(\frac{d\Theta}{dR^{*}}\right)^{2}+\frac{Br\tau^{*}_{r\theta}}{\Omega(\Pi-1)}R^{*}\frac{d}{dR^{*}}\left(\frac{V_{\theta}}{R^{*}}\right). \quad (32)$$

In Eq. (32), is the non-dimensional temperature difference. For the isothermal case it is defined as $\Delta T/T_i$ also the isoflux case $\Omega=qR_i/kT_i$. Also, Br/Ω is a group parameter that determines the relative importance between viscous dissipation and heat conduction effects.

By substituting non-dimensional temperature and velocity profile in Eq. (32), the entropy generation number (N_s) for both boundary conditions is derived as:

$$N_{sT}=F_{1}+\frac{1}{64}\left(F_{2}+F_{3}+\frac{F_{4}+F_{5}+F_{6}+F_{7}}{F_{8}}\right), \quad (33)$$

$$N_{sq}=F_{1}+\frac{1}{64}\left(F_{2}+F_{3}+F_{9}\right). \quad (34)$$

Descriptions of terms F_1, F_2 etc are given in the Appendix. F_1 is fluid friction contribution which is unchanged for both thermal boundary conditions because the flow and thermal fields are independent of each other.

Fluid versus heat transfer irreversibility

The first term in Eq. (32) which is due to heat transfer is shown as N_R, and the second term which is due to fluid friction as N_F.

$$N_{R}=\left(\frac{d\Theta}{dR^{*}}\right)^{2}, \quad (35\text{-}a)$$

$$N_{F}=\frac{Br\tau^{*}_{r\theta}}{\Omega(\Pi-1)}R^{*}\frac{d}{dR^{*}}\left(\frac{V_{\theta}}{R^{*}}\right). \quad (35b)$$

The ratio of entropy generation due to heat transfer to total entropy generation is called Bejan number (Be) which presents the irreversibility distribution and can be defined as follows [36]:

$$Be=\frac{N_{R}}{N_{R}+N_{F}}. \quad (36)$$

The Bejan number ranges from 0 to 1. When *Be=0*, the total generated entropy is arising from fluid friction, and when *Be=1* means that the total entropy is produced just by heat transfer. For the same contribution of heat transfer and fluid friction to irreversibility, Bejan's number is equal to *1/2*. By using Eqs. (33 and 36), the following equation for Bejan number in the case of isothermal boundary conditions is obtained as follows:

$$Be_{T}=\frac{\frac{1}{64}\left(F_{2}+F_{3}+\frac{F_{4}+F_{5}+F_{6}+F_{7}}{F_{8}}\right)}{F_{1}+\frac{1}{64}\left(F_{2}+F_{3}+\frac{F_{4}+F_{5}+F_{6}+F_{7}}{F_{8}}\right)}, \quad (37)$$

Also, the Bejan number for isoflux boundary condition is derived by substituting Eq. (34) in Eq. (36) as follows:

$$Be_{q}=\frac{\frac{1}{64}\left(F_{2}+F_{3}+F_{9}\right)}{F_{1}+\frac{1}{64}\left(F_{2}+F_{3}+F_{9}\right)}. \quad (38)$$

Global Entropy Generation

The volumetric average entropy generation rate ($[N_s]_{av}$) is defined:

$$\left[N_{s}\right]_{av}=\frac{1}{\forall}\int N_{s}d\forall=\frac{1}{\forall}\int N_{s}r\,d\theta\,dr\,dz, \quad (39)$$

By substituting Eqs. (33 and 34) in Eq. (40) and then integration, the average entropy generation rate can be obtained.

$$[N_s]_{av} = \frac{2}{\Pi^2 - 1}\int_1^{\Pi} N_s R^* \, dR^*. \quad (40)$$

Numerical integration is used for determining the average entropy generation rate.

Validation

Due to the simple rheological model of Newtonian fluids, the obtained equations for hydrodynamics and heat transfer solutions of Newtonian fluids can be followed easily. The Giesekus model becomes simple to Newtonian by setting α and De as zero. Therefore, one should expect that the results obtained for Giesekus fluids tend to those of Newtonian when and De have very small values. This is a way for validation results of complex fluids. The results of Newtonian fluid for velocity and temperature profiles also entropy generation and Bejan numbers, which are reported in [19,27] are compared with the results of this study. As seen in Fig. 2, there is high compliance between the results obtained by two solutions.

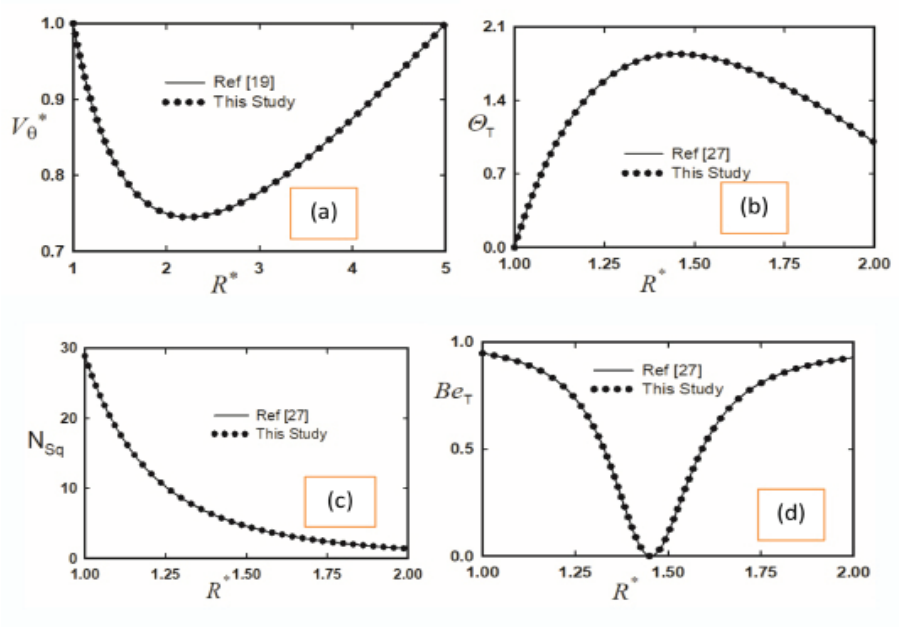

Fig. 2 Comparison between Giesekus model at De=0.01 and α=0.05 in this study and Newtonian fluid for a-Velocity profile in [19] at Π=5 and β =1 b-Temperature profile in [27] at Π=2, β =1, and Br=6 c-Entropy generation number in [27] at Π=2, β =0, and Br=1 d- Bejan number in [27] at Π=2, β =1, and Br=6 and Br/Ω.

Results and Discussions

In Fig.3a, the non-dimensional temperature profiles for isothermal boundary conditions with different Brinkman numbers are shown. The temperature profiles are nearly linear in shape for rather small values of Brinkman numbers, but for *Br* >*2*, they exhibit a maximum value within the annular gap. The reason for this happening is argued as follows: by increasing Brinkman's number, the viscous dissipation effect, and thereby internal generated heat increases, which causes an increase in temperature, but the wall temperature is fixed. Thus, at *Br*>*2*, the fluid temperature will become higher than the warmer wall temperature, and a maximum is observed. The maximum point is important because the entropy generation due to heat transfer is zero (*Be=0*) at this point.

In Fig. 3b, a non-dimensional temperature profile at different values of Deborah number (*De*) is illustrated. By increasing elasticity due to the shear-thinning behavior of Giesekus fluid, the effect of viscous dissipation decreases. In the high values of *De*, viscous dissipation is negligible, and therefore, the fluid temperature starts to warm monotonically from the inner cylinder to the outer one. But in an insignificant value of elasticity (e.g. *De*=0.1), the viscous dissipation effect is significant, and a maximum value of temperature profile can be observed within the annular gap. The effects of Brinkman number (*Br*) and Deborah number (*De*) on the non-dimensional temperature for isoflux boundary conditions are shown in Figures 4a and 4b, respectively. By increasing *Br*, the temperature gradient increases similar to the isothermal case, and elasticity increase acts similar to Brinkman number decreasing.

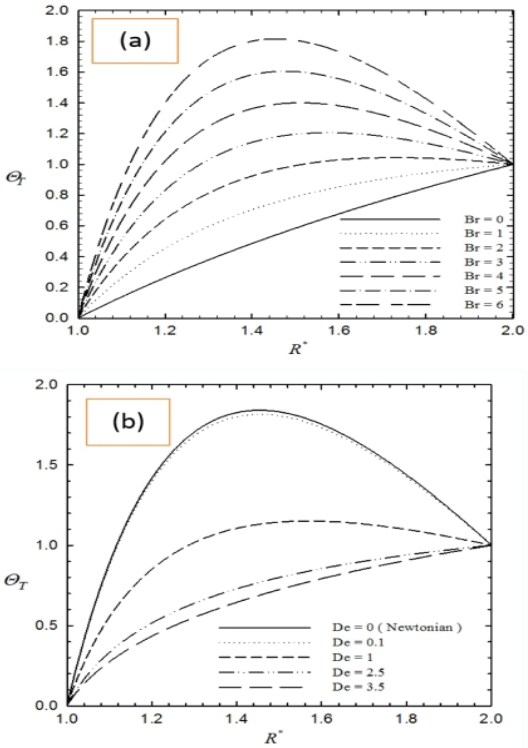

Fig. 3 Temperature profiles for isothermal boundary condition in Π=2, α=0.2 and β=0 for **a**) Different Brinkman numbers at *De*=0.1. **b**) Different Deborah numbers at *Br=6*.

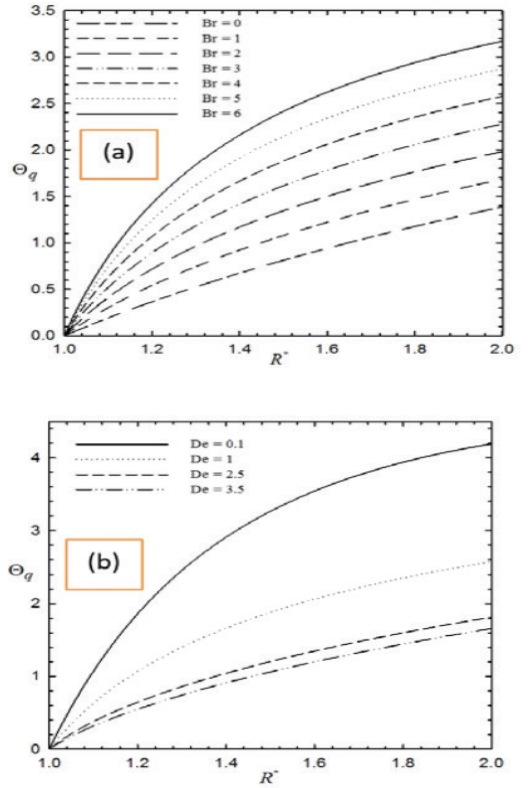

Fig. 4 Temperature profiles for isoflux boundary condition in Π=2, α=0.2 and β=0 for **a**) Different Brinkman number at *De*=1. **b**) Different Deborah numbers at *Br=4*.

In Fig. 5, the effect of group parameter (Br/Ω) in the range of 0 to 1 on entropy generation numbers (N_{sT}, N_{sq}) is shown. Increasing group parameter induced a raise of entropy generation number (N_s) because entropy generation of fluid friction is increased. As seen in Fig. 5, the values of Ns in the inner wall are higher than the outer wall because of the high gradient of temperature as well as the velocity gradient near the inner wall.

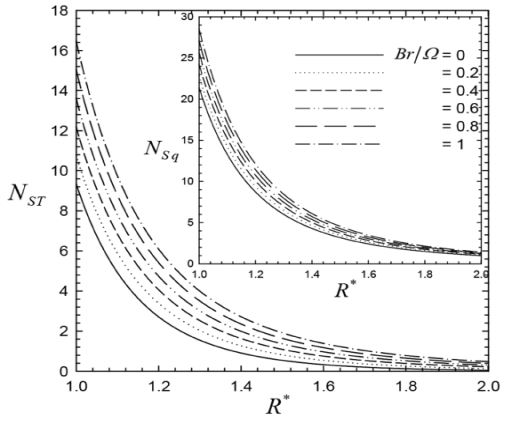

Fig.5 Entropy generation number at different group parameter for *II=2, α=0.2, β*=0, *De*=0.1 and *Br=1*.

In Fig. 6, the effect of velocity ratio (β) on entropy generation number for the two boundary conditions is shown. The behavior is the same for both conditions, except for the magnitude of N_{sq}, which is larger than N_{sT}. By increasing β value, the entropy generation number near the inner wall is reduced. Because by increasing velocity ratio (β),the velocity gradient is decelerated, and thereby, N_F is reduced. Moreover, decreasing the velocity gradient according to Equation 6 decreases the temperature gradient, and thereby NR is reduced. However, this variation is less significant for the central and outer regions of annulus. Profiles approach each other around R*=1.8.

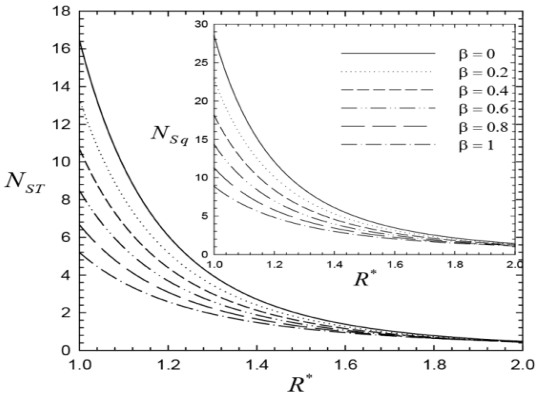

Fig. 6 Entropy generation number at different velocity ratios for *II=2*, α=0.2, *Br/Ω=1*, *De*=0.1 and *Br=1*.

In Fig. 7, the entropy generation numbers (N_{sT} and N_{sq}) for different values of Deborah number (*De*) is shown. Declining trends in N_{sT} and N_{sq} are due to the shear-thinning behavior of Giesekus fluid. Increasing the elasticity will decrease the viscose dissipation effect and temperature gradient. Therefore, both entropy generations, due to the heat transfer (N_R) and fluid friction (N_F) contribution, decrease.

In Fig. 8, variations of Be_T with *R** are given for different values (0-1) of group parameters. The maximum value of the Bejan number occurs at *Br/Ω=1* (i.e., one), which implies that entropy generation due to fluid friction is zero.

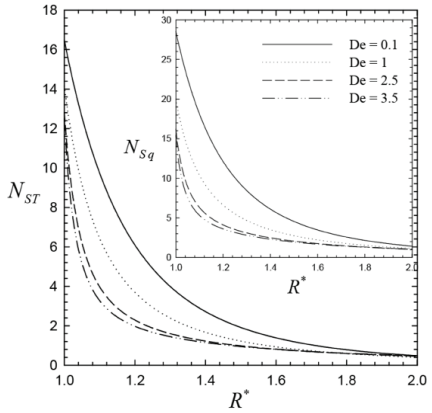

Fig. 7 Entropy generation number at different Deborah numbers for *Π=2, α=0.2, Br/Ω=1, β*=0 and *Br=1*.

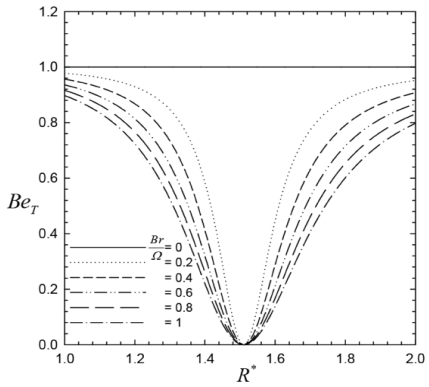

Fig. 8 Bejan number at different group parameters for *Π=2, α=0.2* and *β*=0, *De*=0.1 and *Br=4*.

Bejan number decreases by group parameter growth that indicates an increase in viscous dissipation contribution to entropy generation. All profiles show a minimum point inside the annular gap due to the existence of a maximum point in the temperature distribution. At maximum temperature, the temperature gradient is zero ($\partial\Theta/\partial R^*=0$), and thereby N_R equals 0 (N_R =0). Hence, in R^*=1.51, all of the group parameter profiles have Be=0, which shows at this point, only fluid friction produces the entropy.

In Fig. 9, Be_T as a function of R^* for the various value of velocity ratio (β) is shown. Because of higher temperature and velocity gradients near the inner wall, the maximum value of irreversibility due to heat transfer for all values of occurs on the inner wall. It is also apparent that all profiles intersect with each other around $R^* \approx 1.2$. At this point, where $\beta \leq 1$, all profiles have the same contribution of heat transfer to entropy generation. Furthermore, the location of this point changes by a change in the Brinkman number. The minimum value of profiles, which shows the dominant contribution of fluid friction to entropy generation, shifts towards the outer wall by increasing . This minimum occurs in the outer wall at β =1.

In Fig. 10, the Bejan number (Be_T) profile for different values of *Br* is shown. As stated in section 4.1 for $Br < 2$ and in this case for *Br*=1, the Bejan profiles don't show any minimum points because in temperature distribution, no peak is observed. The profiles intersect each other around R^*=1.35 where the heat transfer contribution of total generated entropy is the same for all Brinkman numbers.

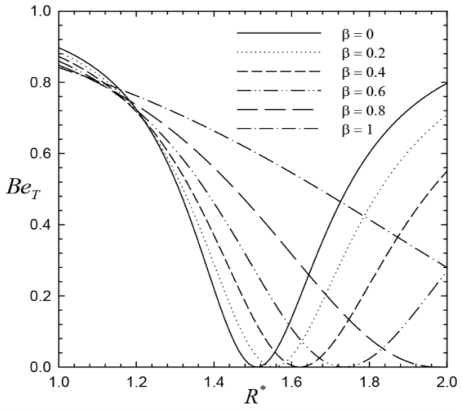

Fig. 9 Bejan number at different velocity ratios for *Π=2*, α=0.2, *Br/Ω=1*, *De*=0.1 and *Br*=4.

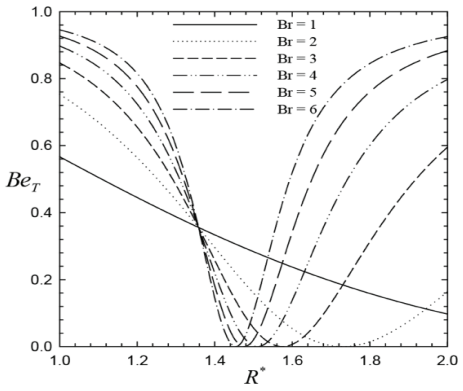

Fig. 10 Bejan number at different Brinkman numbers for *Π=2*, α=0.2, *Br/Ω=1*, *β*=0 and *De*=0.1.

As can be seen for the reduction of the Brinkman number, the minimum point shifts towards the outer wall.

In Fig. 11, the effect of fluid elasticity (*De*) on the Bejan number (Be_T) is shown. For small values of fluid elasticity, the Bejan number drops through the annular gap, and after reaching a minimum at Be_T=0, again, it increases towards the outer cylinder and the minimum point shifts toward the outer wall by increasing elasticity. But for higher values of elasticity, there is no minimum inside the annular gap because of the absence of a maximum point in the temperature distribution.

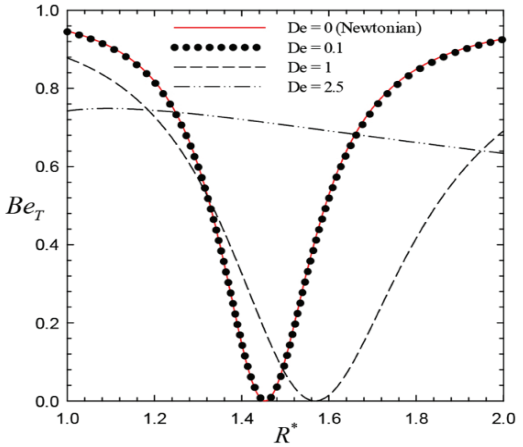

Fig. 11 Bejan number at different Deborah number for *Π=2*, α=0.2, *Br/Ω=1*, *β*=0 and *Br*=6.

In Fig. 12, the effect of group parameter (Br/Ω) on the average entropy generation rate ($[N_s]_{ave}$) for the isothermal case is displayed. By increasing the group parameter, $[N_{ST}]_{ave}$ increases. A minimum point at β=2 is observed, the magnitude of this point equals to $[Ns_T]_{ave} \approx 0.9618$, for all values of Br/Ω.

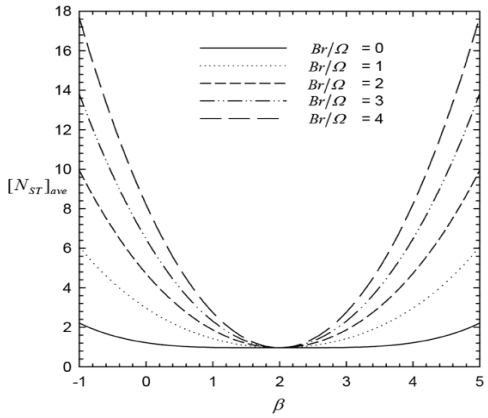

Fig. 12 Average entropy generation profiles for different group parameters for Π=2, α=0.2, De=0.1 and Br=1.

Average entropy generation is plotted in Fig. 13 versus β for various values of Brinkman number. By increasing Br, average entropy generation rate increases. Similar to Fig. 12, for each Br, profiles are symmetrical around β=2.

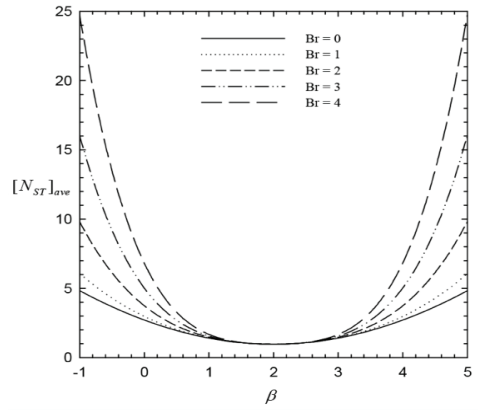

Fig. 13 Average entropy generation profiles at different Brinkman numbers for Π=2, α=0.2, De=0.1 and Br/Ω=1.

According to Figs. 12 and 13, the location of the minimum point of profiles is independent of Brinkman number (Br) and group parameter (Br/Ω), and for Π=2 it is at β=2 for both figures. In other words, this minimum point occurs when $\beta=\Pi$. At this point, no relative angular motion exists between the inner and outer cylinders (i.e. $\omega_i = \omega_0$). In fact, the annulus and the contained fluid act as a rotating solid body. At this condition, the shear stress ($\tau^*_{r\theta}$ or τ^*_{wi}) and the entropy generation due to viscous dissipation is zero.

By substituting $\tau^*_{wi}=0$, in Equations 33 and 34 and then by putting them in Equation 40 and integrating, the following equations for the minimum average entropy generation rate ($[N_S]_{av,min}$) can be obtained:

$$[N_{ST}]_{ave,min} = \frac{2}{(\Pi^2-1)Ln\,\Pi}, \qquad [N_{Sq}]_{ave,min} = \frac{2\Pi^2 Ln\,\Pi}{\Pi^2-1}. \quad (41)$$

A similar result has been reported by Mahmud and Fraser [19] for Newtonian fluid and Mirzazadeh et al. [27] for sPTT fluid. The minimum average entropy generation rate ($[N_{ST}]_{av,min}$, and $([N_{Sq}]_{av,min}$) as a function of Π is plotted in Fig. 14. Moreover, the minimum average entropy generation rates at Π=1.763 are the same and equal to 1.678 for both boundary conditions.

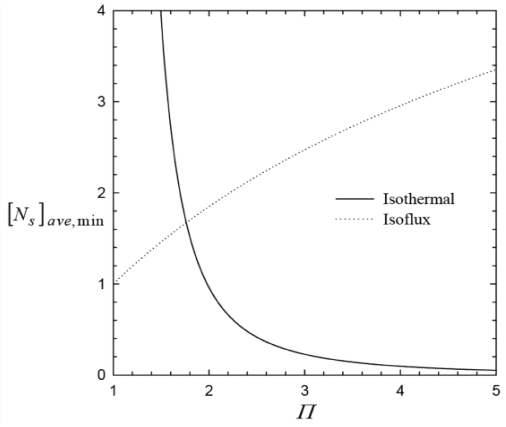

Fig. 14 Minimum average entropy generation profiles.

In Fig. 15, the distribution of average entropy generation rate as a function of Deborah number at different mobility factors (α) for isothermal boundary condition is shown. By increasing elasticity (α and De), $[N_s]_{ave}$ decreases due to the shear-thinning behavior of Giesekus fluid.

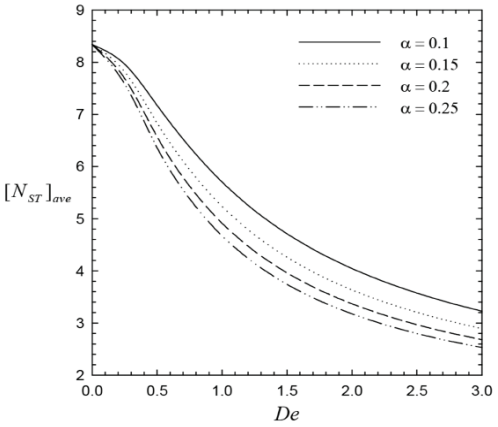

Fig. 15 Average entropy generation profiles at different Brinkman numbers form Π=2, Br=1, β=0 and Br/Ω=4.

Conclusions

The entropy analysis and convective heat transfer of Giesekus viscoelastic fluid were studied in a gap between two rotating cylinders. Two different types of boundary conditions are considered: (a) the constant and different temperature at walls, (b) constant heat flux at the outer wall, and constant temperature at the inner wall. The governing equations are solved by the analytical approach, and subsequently, the expressions for non-dimensional temperature, entropy

generation, and Bejan numbers are derived, and then the effects of elasticity and viscous dissipation parameters along with the geometric parameter are investigated on them. The entropy generation rates (N_s) in the inner wall are higher than the outer wall because of the high gradient of temperature and velocity near the inner wall. By increasing the group parameter (Br/Ω) and Brinkman number (Br), the entropy generation number is increased; therefore, they are the undesirable parameters for the system and increase the operating cost of the system. But increment of fluid elasticity (De and α) and velocity ratio (β) decreases the entropy generation number and, consequently, operating cost; thus, they are the desired parameters for the system. Moreover, all the Bejan number profiles show a minimum point inside the annular gap due to the existence of a maximum point in the temperature distribution. Also, the maximum value of the Bejan number is one. It indicates that there is no contribution of fluid friction to entropy generation, and the minimum value of the Bejan number is zero, which indicates that the entropy generation is only influenced by fluid friction. Ultimately, according to this study, it is found out that the location of the minimum average entropy generation rate depends only on the velocity ratio (β) and occurs at $\beta=\Pi$ where no relative angular motion exists between two cylinders.

Nomenclatures

Capital Letters

Be: Bejan number
Br: Brinkman number
C: Integration constant
De: Deborah number ($\lambda u_c/\delta$)
N_F: Entropy generation number; fluid friction contribution
N_R: Entropy generation number; radial heat transfer contribution
N_S: Entropy generation number; total
R: Radius (m)
S_G: Entropy generation rate, Watt/m^3.K
$S_{G,c}$: Characteristic entropy generation rate
T: Temperature (K)
V: Velocity (ms^{-1})

Lowercase Letters

C_p: Specific heat at constant pressure (g/Kg.K)
k: Thermal conductivity (watt/m k)
q: Heat flux (w/m^2)
r: Radial coordinate (m)
t: Time (s)
uc: Characteristic velocity

Greek Symbols

α: Mobility parameter of Giesekus
β: Velocity ratio ($\omega_0 R_0 / \omega_i R_i$)
δ: Annular gap (R_0-R_i)
Φ: Viscous dissipation function
$\dot{\gamma}$: Shear rate tensor (s−1)
η: Zero shear viscosity (Pa s)
φ: The ratio of outer and inner wall heat fluxes
Φ: Viscous dissipation term
ϑ: Convected derivative
λ: Zero shear relaxation time (s)
ρ: Fluid density (kg/m^3)
Π: Radius ratio (R_0/R_i)
Θ: Non-dimensional temperature
τ: Stress tensor (Pa)
Ω: Non-dimensional temperature difference
ω: Angular velocity (Rad/s)
$\forall$: The volume of the annular gap (m3)

Superscripts

T: Transpose of tensor
*: Refers to non-dimensional quantities

Subscripts

av: Refers to the average value
i: Refers to the inner cylinder
o: Refers to the outer cylinder
w: Refers to wall value

Appendix

$$F_1=\frac{\mathrm{Br}\,\tau_{wi}^{*\,2}}{\Omega(\Pi-1)^2}\left(\frac{R^{*4}+X^2(1-2\alpha)}{(R^{*4}-X^2)^2}\right),$$

$$F_2=\frac{4BrR^*\tau^2(1-\alpha)}{(\Pi-1)^2(R^{*4}-X^2)},$$

$$F_3=\frac{2\sqrt{\alpha}Br\tau_{wi}^*\left[Log\left(\frac{X+R^{*2}}{X-R^{*2}}\right)\right]}{(\Pi-1)^2DeR^*},\quad F_4=8\sqrt{\alpha}De\,(\Pi-1)^2,$$

$$F_5=Br\tau_{wi}^*(\alpha-1)Log\left(\frac{(\Pi^2-X)(1+X)}{(1-X)(\Pi^2+X)}\right),$$

$$F_6=\alpha Br\tau_{wi}^*\left[PolyLog\left(2,\frac{1}{X}\right)-PolyLog\left(2,-\frac{1}{X}\right)\right],$$

$$F_7=\alpha Br\tau_{wi}^*\left[PolyLog\left(2,-\frac{\Pi^2}{X}\right)-PolyLog\left(2,\frac{\Pi^2}{X}\right)\right],$$

$$F_8=\sqrt{\alpha}DeR^*Log(\Pi)(\Pi-1)^2,$$

$$F_9=\frac{8\Pi}{R^*}\left(1+Br\tau_{wi}^{*\,2}\left(\frac{\Pi^2(\alpha-1)}{2(\Pi^4-X^2)\Pi(\Pi-1)^2}-\frac{\sqrt{\alpha}\,arctanh\left(\frac{\Pi^2}{X}\right)}{2De\tau_{wi}^*\Pi(\Pi-1)^2}\right)\right).$$

Reference

1. Mohseni MM, Rashidi F (2017) Analysis of axial annular flow for viscoelastic fluid with temperature dependent properties, International Journal of Thermal Sciences, 120: 162-174.
2. Riaz A, Zeeshan A, Ahmad S, Razaq A, Zubair M (2019) Effects of external magnetic field on non-newtonian two phase fluid in an annulus with peristaltic pumping, Journal of Magnetics, 24, 1: 62-69.
3. Abdelmalek Z, Khan SU, Waqas H, Riaz A, Khan IA, Tlili I (2020) A mathematical model for bioconvection flow of Williamson nanofluid over a stretching cylinder featuring variable thermal conductivity, activation energy and second-order slip, Journal of Thermal Analysis and Calorimetry, 1-13.

4. Mohseni MM, Tissot G, Badawi M (2020) Effects of wall slip on convective heat transfers of giesekus fluid in microannulus, Journal of Heat transfer, 142: 8.
5. Mohseni MM, Rashidi F (2015) Axial annular flow of a Giesekus fluid with wall slip above the critical shear stress, Journal of Non-Newtonian Fluid Mechanics, 223: 20-27.
6. Riaz A, Gul A, Khan I, Ramesh K, Khan SU, Baleanu D, Nisar KS (2020) Mathematical analysis of entropy generation in the flow of viscoelastic nanofluid through an annular region of two asymmetric annuli having flexible surfaces, Coatings, 10, 3: 213.
7. Riaz A, Razaq A, Awan AU (2017) Magnetic field and permeability effects on Jeffrey fluid in eccentric tubes having flexible porous boundaries, Journal of Magnetics, 22, 4: 642-648.
8. Tong, AT, Yu M, Ozbayoglu E, Takach N (2020) Numerical simulation of non-Newtonian fluid flow in partially blocked eccentric annuli, Journal of Petroleum Science and Engineering, 107368.
9. Mohseni MM, Rashidi F, (2010) Viscoelastic fluid behavior in annulus using Giesekus model, Journal of non-newtonian fluid mechanics, 165, 21-22: 1550-1553.
10. Hashemabadi S, Mirnajafizadeh S (2010) Analysis of viscoelastic fluid flow with temperature dependent properties in plane Couette flow and thin annuli, Applied mathematical modelling, 34, 4: 919-930.
11. Giesekus H (1982) A simple constitutive equation for polymer fluids based on the concept of deformation-dependent tensorial mobility, Journal of Non-Newtonian Fluid Mechanics, 11, 1-2: 69-109.
12. Jouyandeh M, Mohseni MM, Rashidi F (2017) Tangential flow analysis of giesekus model in concentric annulus with both cylinders rotation, Journal of Applied Fluid Mechanics, 10: 6.
13. Jouyandeh M, Mohseni MM, Rashidi F (2014) Forced convection heat transfer of Giesekus viscoelastic fluid in concentric annulus with both cylinders rotation, Journal of Petroleum Science and Technology, 4, 2: 1-9.
14. Sonntag RE, Borgnakke C, Van Wylen GJ (1998) Fundamentals of thermodynamics, 6th ed., Wiley, New York, 1-2257.
15. Bejan A (1979) A study of entropy generation in fundamental convective heat transfer, Journal of Heat Transfer, 101, 4: 718-725.
16. Bejan A (1982) Second-law analysis in heat transfer and thermal design, Advances in Heat Transfer, 15, 1: 1-58.
17. Yilbas BS (2001) Entropy analysis of concentric annuli with rotating outer cylinder, Exergy, An International Journal, 1, 1: 60-66.
18. Mahmud S., Fraser RA (2002) Second law analysis of heat transfer and fluid flow inside a cylindrical annular space, Exergy, An International Journal, 2, 4: 322-329.
19. Mahmud S, Fraser RA (2003) Analysis of entropy generation inside concentric cylindrical annuli with relative rotation. International Journal of Thermal Sciences, 42, 5: 513-521.
20. Mahmud S, Fraser RA (2006) Second law analysis of forced convection in a circular duct for non-Newtonian fluids, Energy, 31, 12: 2226-2244.
21. Mahian O, Mahmud S, Pop I (2012) Analysis of first and second laws of thermodynamics between two isothermal cylinders with relative rotation in the presence of MHD flow, International Journal of Heat and Mass Transfer, 55, 17-18, 4808-4816.
22. Mahian O, Oztop H, Pop I, Mahmud S, Wongwises S (2013) Entropy generation between two vertical cylinders in the presence of MHD flow subjected to constant wall temperature. International communications in heat and mass transfer, 44: 87-92.
23. Mahian O, Oztop HF, Pop I, Mahmud S, Wongwises S (2013) Design of a vertical annulus with MHD flow using entropy generation analysis, Journal of Thermal Science, 17, 4: 1013-1022.
24. Kahraman A., Yürüsoy M (2008) Entropy generation due to non-Newtonian fluid flow in annular pipe with relative rotation: constant viscosity case, Journal of Theoretical and Applied Mechanics, 46, 1: 69-83.
25. Yilbas BS, Yürüsoy M, Pakdemirli M (2004) Entropy analysis for non-Newtonian fluid flow in annular pipe: constant viscosity case, Entropy, 6, 3: 304-315.
26. Yürüsoy M, YilbaŞ B, Pakdemirli M (2006) Non-Newtonian fluid flow in annular pipes and entropy generation: temperature-dependent viscosity. Sadhana, 31, 6: 683-695.
27. Mirzazadeh M, Shafaei A, Rashidi F (2008) Entropy analysis for non-linear viscoelastic fluid in concentric rotating cylinders, International Journal of Thermal Sciences, 47, 12: 1701-1711.
28. Mohseni MM, Rashidi F (2015) Second law analysis of Giesekus viscoelastic fluid for axial annular flow, International Journal of Exergy, 16, 4: 404-429.
29. Riaz A, Bhatti MM, Ellahi R, Zeeshan A, and Sait MS (2020) Mathematical analysis on an asymmetrical wavy motion of blood under the influence entropy generation with convective boundary conditions, Symmetry, 12, 1: 102.
30. Mohseni MM, Rashidi F, Movagar MRK (2015) Analysis of forced convection heat transfer for axial annular flow of Giesekus viscoelastic fluid, Korean Chemical Engineering Research, 53, 1, 91-102.
31. Mohseni MM, Tissot G, Badawi M (2018) Forced convection heat transfer of Giesekus fluid with wall slip above the critical shear stress in pipes, International Journal of Heat and Fluid Flow, 71, 442-450.
32. D'Alessandro G, de Monte F (2019) Optimal experiment design for thermal property estimation using a boundary condition of the fourth kind with a time-limited heating period, International Journal of Heat and Mass Transfer, 134, 1268-1282.
33. Giesekus H (1983) Stressing behaviour in simple shear flow as predicted by a new constitutive model for polymer fluids, Journal of non-newtonian fluid mechanics, 12, 3: 367-374.
34. Bird RB, Armstrong RC, Hassager O (1987) Dynamics of polymeric liquids, Fluid mechanics, 1.
35. Bejan A (2013) Entropy generation minimization: the method of thermodynamic optimization of finite-size systems and finite-time processes, CRC press.
36. Paoletti S, Rispoli F, Sciubba E (1989) Calculation of exergetic losses in compact heat exchanger passages, in ASME AES.